L.9: X-ray topography for imaging structural defects in single crystals

Structural defects in single crystals, particularly the type of defects, their spatial distribution, and the history of generation and propagation during growth, has strong linkage with the quality of the grown crystal and their influence on the physical properties. In order to map spatial and temporal profile of these defects in the crystals grown in the Laser Materials Development and Devices Division (LMDDD), a digital X-ray topographic imaging facility has been established. The topography system consists of microfocus X-ray generator (Cu anode), goniometer, sample stage, CCD detector and software modules to acquire and process the imaging data. The photograph of the system is shown in Fig L.9.1 (a, b).

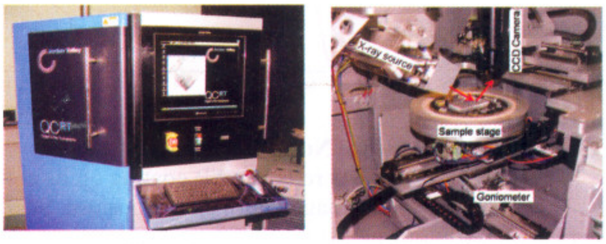

(a) (b)

Fig L.9.1. (a) Digital X-ray topography system and (b) different parts of the system.

The X-ray topographic imaging is based on the diffraction of X-rays by lattice planes satisfying the Bragg's condition. Around structural defect the planes are tilted from their ideal orientations, resulting in low intensity of diffracted X-rays as compared to regions without (or less) defects. Thus a varying intensity contrast is recorded by the detector which represents the defect structure of the crystal under study. We have studied defect structure of some crystals grown in the Division such as large size potassium dihydrogen phosphate (KDP) crystals, lithium niobate (LN) crystals, lithium tetra borate, lithium iodate etc. Fig. L.9.2 shows the large size KDP crystal and an X-ray topograph of a plate taken from its central part. The prismatic sector is more severely affected by dislocations as compared to pyramidal sector.

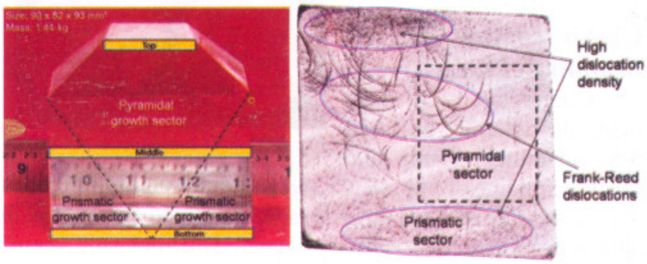

Fig L.9.2. Large size KDP crystal and X-ray topograph of (316) planes for plate from middle of the crystal.

The topograph of the bottom plate (Fig. L.9.3a) showed the process of dislocations originating from seed crystal and their propagation during growth. The topograph of the top plate (Fig. L.9.3b) was found to have relatively lesser dislocations, indicating that the technique of terminating the growth using solution-air interface does not introduce any defects in the crystal.

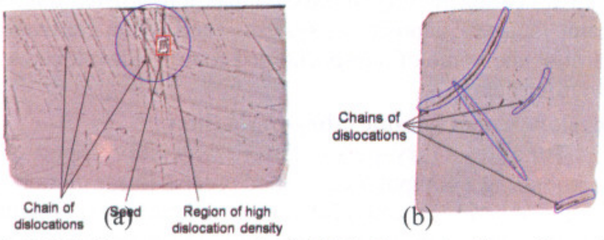

Fig L.9.3. X-ray topograph of (316) planes in plates from the bottom and top portion of the KDP crystal.

A lithium iodate crystal and its topograph showing growth sector boundaries and striations is shown in Fig L.9.3a. A lithium tetra borate crystal and its topograph showing inclusion and dislocations is shown in Fig L.9.4b. A lithium niobate crystal and its topograph showing misoriented regions w.r.t. the diffracting planes is shown in Fig L.9.4c.

(a)

(b)

(c)

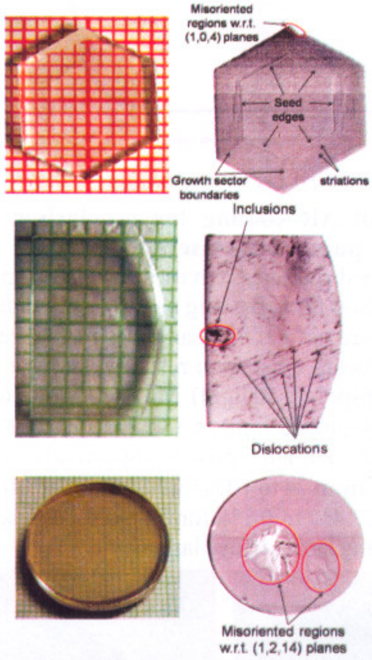

Fig L.9.4. (a) $LiIO_3$ crystal oriented along [001] and topograph taken for (104) planes, (b) $Li_2B_4O_7$ crystal oriented along [100] and topograph taken for (100) planes, and (c) $LiNbO_3$ crystal sample oriented along [001] and topograph taken for (12 14) planes.

Reported by:
Sunil Verma (sverma@rrcat.gov.in), S.K. Sharma, and K.S. Bartwal